analytical chemistry

pubs.acs.org/ac Article

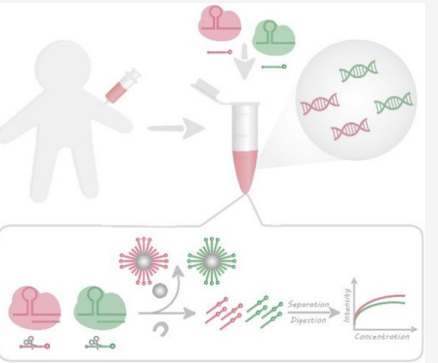
CRISPR-Cas12a/Cas13a Multiplex Bioassay for ctDNA and miRNA by Mass Spectrometry

Yan Li, Yichen Li, Yueli Hu, Rui Liu,* and Yi Lv*

Cite This: https://doi.org/10.1021/acs.analchem.4c05961 Read Online

ACCESS | Metrics & More | Article Recommendations | Supporting Information

ABSTRACT: The CRISPR-Cas system, particularly CRISPR-Cas12a and CRISPR-Cas13a, has been widely utilized in constructing various biosensors due to their "*trans*-cleavage" ability as a means of signal amplification. However, this universal "*trans*-cleavage" characteristic also presents a challenge for realizing CRISPR-Cas multiplexed bioanalysis. Besides, potential signal cascading interference and complicated design are notable obstacles in CRISPR-Cas multiplexed bioanalysis. Herein, we propose a mass spectrometry method that leverages the CRISPR-Cas12a/13a system to achieve simultaneous detection of ctDNA and miRNA. Based on the properties of the CRISPR-Cas12a/13a system, two types of nanoparticle reporter probes have been engineered, using cancer-related biomarkers ctDNA and miR-21 as our model analytes. The nanoparticle tags, which intrinsically incorporated millions of detectable atoms, combined with the CRISPR-Cas12a/Cas13a system's "*trans*-cleavage" ability, allow the proposed mass spectrometry strategy to achieve fmol-level detection limits without any nucleic acid amplification procedures. The assay was successfully applied to human serum samples, demonstrating its potential for early disease diagnosis and progression tracking.



Downloaded via SHANGHAI NORMAL UNIV on February 23, 2025 at 00:43:16 (UTC).
See https://pubs.acs.org/sharingguidelines for options on how to legitimately share published articles.

Clustered regularly interspaced short palindromic repeats (CRISPR) and their associated proteins (Cas) collectively form the CRISPR-Cas system,[1,2] which has rapidly captured the world's imagination as a groundbreaking tool for gene editing and epigenetic regulation.[3,4] Over the past few years, the CRISPR-Cas system, especially CRISPR-Cas12a and CRISPR-Cas13a, has emerged as a potent tool for biomolecular diagnostics, due to their "*trans*-cleavage" ability, which is particularly effective in detecting nucleic acid molecules like circulating tumor DNA (ctDNA) and microRNAs (miRNA), as well as other non-nucleic acid biomolecules.[5−7] With the guidance of crRNA, the Cas protein rapidly recognizes and binds to its target, initiating the activation of either the CRISPR-Cas12a or the CRISPR-Cas13a system. This activation subsequently prompts the Cas protein to perform collateral cleavage, a mechanism that cleaves adjacent ssDNA or ssRNA in a nonspecific manner to amplify the signal.[8,9] However, the "*trans*-cleavage" mechanism of the CRISPR-Cas system is also constrained to the analysis of single-target biomolecules in one test, posing a challenge to multiplexed bioanalysis.[10,11]

In recent years, scientists utilized the properties of CRISPR/Cas in combination with fluorescence, microfluidics, and other technologies to realize CRISPR-Cas multiplexed bioanalysis.[12,13] In 2018, Zhang et al. proposed an approach utilizing the distinct base-cleavage preferences of various Cas13 protein subtypes to enable multiplexed detection within the CRISPR-Cas system.[14,15] Furthermore, the incorporation of separation methods such as microfluidics also facilitated the pursuit of multiplexed detection using the CRISPR-Cas system.[16,17] Leveraging the "cis-cleavage" activity of CRISPR-Cas9 and incorporating protospacer adjacent motif (PAM) sequences provide an effective approach to enable CRISPR-Cas multiplexed bioanalysis.[18] Despite these encouraging achievements, research on CRISPR-Cas multiplexed bioanalysis is still rare, with signal crosstalk and the complicated design of PAM posing as significant bottlenecks. Consequently, there is an urgent need for a CRISPR-Cas-enabled multiplexed bioanalysis assay that is simple, quick, highly efficient, and cost-effective.

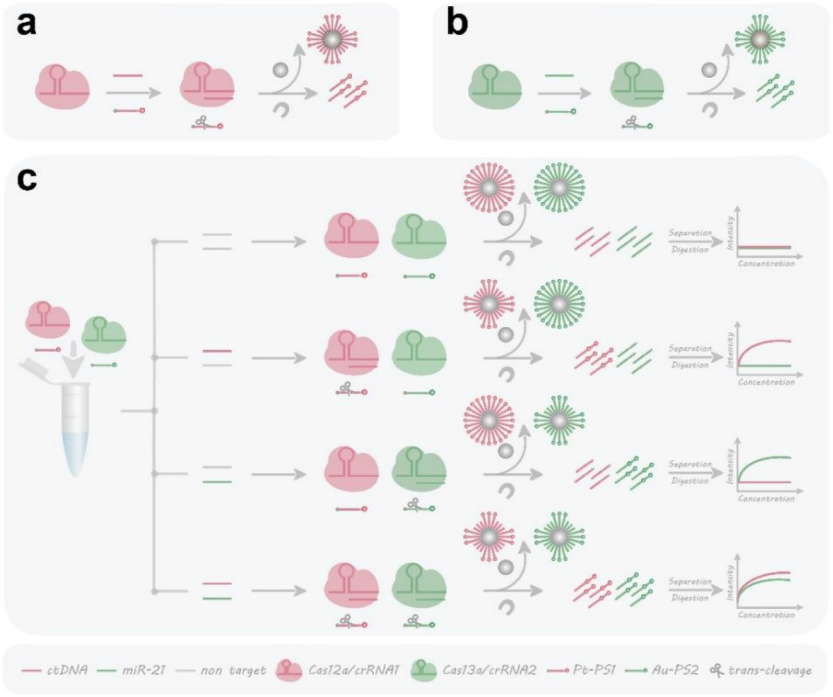
The accelerating development of metal element tags capable of various mass spectrometry methods, without the hindrance of spectral overlap interference, has substantially addressed the current need for advancements in multiplexed bioanalysis.[19,20] Additionally, the ability of mass cytometry (CyTOF), inductively coupled plasma mass spectrometry (ICP-MS), and other mass spectrometry methods to support simultaneous, rapid, high-throughput, and high-sensitivity analysis of multiple elements contributes enormous potential to multiplexed bioanalysis.[21−24] Currently, metal element labeling methods can be broadly categorized into lanthanide labeling

Received: November 5, 2024
Revised: February 12, 2025
Accepted: February 14, 2025

© XXXX American Chemical Society

https://doi.org/10.1021/acs.analchem.4c05961
Anal. Chem. XXXX, XXX, XXX−XXX

Scheme 1. Multiplexed Detection Mechanism of ctDNA and miRNA Utilizing CRISPR-Cas12a/Cas13a Integrated with ICP-MS[a]



[a](a) Activation of CRISPR-Cas12a by ctDNA, triggering cleavage of the DNA reporter probe Pt-PS1. (b) Activation of CRISPR-Cas13a by miR-21, triggering cleavage of the RNA reporter probe Au-PS2. (c) CRISPR-Cas12a/Cas13a dual-targeting behavior under multiple conditions: absence of both ctDNA and miR-21, presence of only ctDNA, presence of only miR-21, and presence of both ctDNA and miR-21.

utilizing macrocyclic compounds, metal-containing nanoparticles, metal nanocluster labeling, and polymeric element tags.[25,26] Utilizing various metal element tags for multiplexed bioanalysis offers high-throughput, cost-effectiveness, and multibiomarker analysis in one run, making it ideal for complex sample analysis. This has been applied to the detection of multiple nucleic acids,[27−30] proteins,[31−33] enzymes,[34] small biological molecules,[35] and even facilitating single-cell analysis.[36−39] Despite the great potential, it is still challenging to establish a sensitive mass spectrometric CRISPR-Cas multiplex bioassay, mainly due to two obstacles: (1) the nonspecific "*trans*-cleavage" characteristic of the CRISPR-Cas system and (2) the sophisticated nanoprobe bioconjugation procedure.

Herein, we developed a mass spectrometry assay that combines CRISPR-Cas12a/Cas13a systems with the sensitivity of nanoparticle labeling, enabling the simultaneous detection of ctDNA and miRNA in a simple and efficient manner (Scheme 1). The ctDNA and miR-21, both of which are closely related to the occurrence of various diseases, are used as model target analytes for analysis.[40,41] Specifically, biotin-modified PS1 DNA and PS2 RNA were labeled onto PtNPs and AuNPs, respectively, to obtain the DNA reporter probe Pt-PS1 and the RNA reporter probe Au-PS2. Once the CRISPR-Cas12a/Cas13a system detects its target analytes, ctDNA and miR-21, it activates the Cas12a and Cas13a enzymes, causing them to selectively cleave the DNA reporter probe Pt-PS1 and the RNA reporter probe Au-PS2, thereby releasing abundant PtNPs and AuNPs into the supernatant. Subsequently, streptavidin-modified magnetic beads (MBs) were employed to separate the uncleaved reporter probes from the cleaved probes,[42,43] which were then processed for detection by ICP-MS. When the target analytes are absent, the CRISPR-Cas12a/Cas13a system remains inactive and yields no signal. The signal intensity measured by ICP-MS is directly proportional to the quantity of metal atoms released into the supernatant, allowing for the accurate quantification of ctDNA and miR-21. Due to the millions of detectable atoms in each nanoparticle tag, and the catalytic *trans*-cleavage ability of the CRISPR-Cas12a/Cas13a system, the proposed ICP-MS strategy provides remarkable sensitivity without any nucleic acid amplification procedures.

EXPERIMENTAL SECTION

Reagents and Apparatus. The signals of ^{195}Pt and ^{197}Au were primarily measured and acquired by inductively coupled plasma mass spectrometry (iQuad ICP-MS, Hengsheng, Beijing, China). Detailed information on the apparatus used for characterization, the materials and reagents employed, the buffers and solutions prepared, as well as the related nucleic acid sequences, can be found in the Supporting Information.

Synthesis of Reporter Probes. The preparation of signal reporter probes, which encompassed platinum nanoparticles modified with PS1 DNA (Pt-PS1) and gold nanoparticles modified with PS2 RNA (Au-PS2), primarily referred to previously reported literature with slight modifications.[44] Diverse PtNPs and AuNPs, categorized by their particle sizes, were placed in a 2 mL centrifuge tube. Following this, Pt-PS1 and Au-PS2, which function as reporter probes modified with varying densities on the nanoparticles, were accomplished by precisely adjusting the ratio of spacer DNA to PS1 DNA/PS2 RNA. After mixing PtNPs with spacer DNA and PS1 DNA, and AuNPs with spacer DNA and PS2 RNA, respectively, they were stored in a freezer at −80 °C for 15

https://doi.org/10.1021/acs.analchem.4c05961
Anal. Chem. XXXX, XXX, XXX−XXX

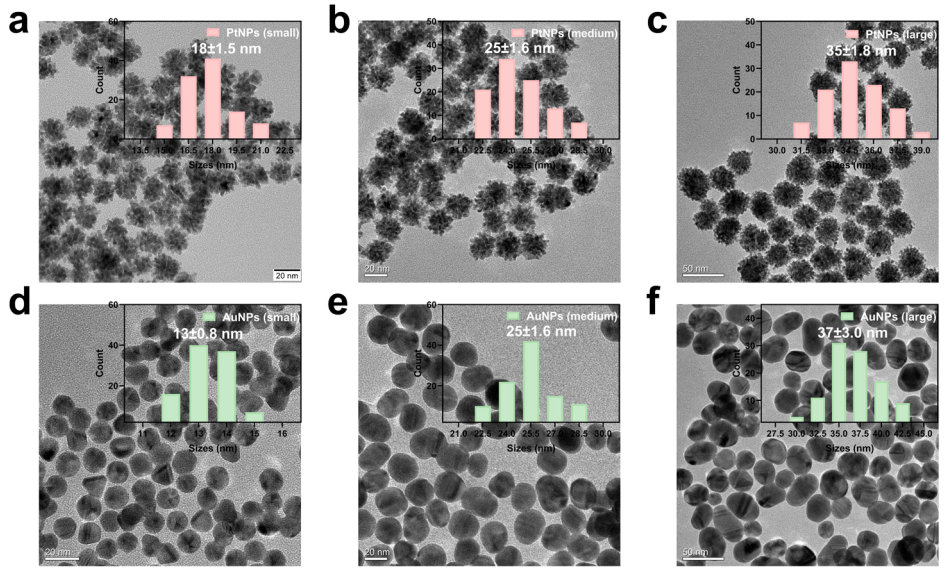


Figure 1. TEM characterization of PtNPs, AuNPs. (a) PtNPs (small size), (b) PtNPs (medium size), (c) PtNPs (large size), (d) AuNPs (small size), (e) AuNPs (medium size), and (f) AuNPs (large size).

min. Thereafter, they were dissolved at room temperature, washed, and centrifuged three times with DEPC H_2O. Finally, they were redissolved separately in 600 μL and 900 μL DEPC H_2O and stored in a refrigerator at 4 °C for future use.

CRISPR-Cas12a/Cas13a for Simultaneous Detection of ctDNA and miRNA. At room temperature, LbCas12a and crRNA1, as well as LbuCas13a and crRNA2, were allowed to preincubate for 20 min, yielding the LbCas12a/crRNA1 and LbuCas13a/crRNA2 binary complexes, respectively. These complexes were subsequently dispensed into 200 μL PCR tubes. Next, 10 μL of Pt-PS1 and Au-PS2 were added, followed by the addition of 5 μL of ctDNA and 5 μL of miR-21. The mixture was then incubated at 37 °C to activate the CRISPR-Cas12a/Cas13a. After 40 min, the reaction was terminated by heating at 65 °C for 5 min to stop the enzymatic cleavage. Notably, Tris-HCl buffer acted as the diluent, solvent, and reaction buffer to guarantee optimal conditions for all Cas proteins involved in the reactions. Once the enzymatic cleavage reaction was terminated, an equal volume of streptavidin-modified magnetic beads diluted in B&W buffer was added, and the mixture was allowed to react at 37 °C for 20 min. Upon completion of magnetic separation, the supernatant was extracted and mixed with aqua regia to digest the CRISPR-Cas12a/Cas13a-specific cleavage products of Pt-PS1 and Au-PS2. This facilitated the release of PtNPs and AuNPs into the supernatant, which were then converted to ^{195}Pt and ^{197}Au ionic signals. After allowing 30 min for digestion, 8 mL of ultrapure H_2O was added, and the mixture was thoroughly mixed and prepared for analysis via ICP-MS.

Gel Electrophoresis and Imaging. Following the blending of the sample and loading buffer at a 1:6 proportion, the mixture was delicately loaded onto a 12% precast-GLgel TBE PAGE. Then, after filling with 1 × TBE buffer, the electrophoresis process began for 30 min at 70 V, followed immediately by 40 min at 90 V. After the electrophoresis was completed, we removed the gel and immersed it in 4s Red Plus nucleic acid stain for an hour to ensure complete staining. Finally, the gel was transferred to the FluoChem M to carry out the imaging process.

Serum Sample Assay. First, the serum was centrifuged at 12,000 rpm and 4 °C for 10 min and then underwent a 100-fold dilution. Following this, it was subjected to further heat inactivation, and the RNase inhibitor was introduced. The mixture was then incubated at 37 °C for 30 min. Ultimately, spiked recovery experiments were performed by adding varying concentrations of ctDNA and miR-21 to the serum samples.

RESULTS AND DISCUSSION

Characterization of Nanoparticles and Reporter probes. The TEM images demonstrate that the prepared PtNPs are composed of three different sizes, with diameters of approximately 18, 25, and 35 nm. In parallel, the AuNPs display particle sizes approximately equal to 13, 25, and 37 nm (Figure 1). For clarity, we categorize the PtNPs/AuNPs into three groups named small, medium, and large PtNPs/AuNPs, based on their particle dimensions. To further investigate this, we applied dynamic light scattering (DLS) to characterize the PtNPs and AuNPs. The results concurred with previous findings, as shown in Figure S1. The preparation of the reporter probe is crafted by leveraging the robust adsorption of polymeric adenine DNA or RNA onto metal nanoparticles under frozen conditions.[44] By adjusting the ratio of spacer DNA to the desired PS1 DNA or PS2 RNA, we can programmatically regulate the surface coverage of PS1 DNA or PS2 RNA on the nanoparticles. The variations in DLS and zeta potential depicted in Figure 2 for PtNPs (medium) vs Pt-PS1 (medium), and AuNPs (small) vs Au-PS2 (low), confirm the successful fabrication of the reporter probes Pt-PS1 (medium) and Au-PS2 (low). Notably, the DLS growth patterns (Figures S2 and S3) observed for PtNPs and AuNPs, along with their respective low-, medium-, and high-density reporter probes (Pt-PS1 and Au-PS2), in conjunction with the zeta potential transitions (Figures S4 and S5) and UV−vis spectral redshifts (Figure S6) documented in the Supporting Information, conclusively demonstrate the successful preparation of these reporter nanoprobes.

Feasibility Investigation. Built upon the discriminative cleavage mechanisms of CRISPR-Cas12a for ssDNA and CRISPR-Cas13a for ssRNA,[8,9] we propose our analytical assay.

https://doi.org/10.1021/acs.analchem.4c05961
Anal. Chem. XXXX, XXX, XXX−XXX

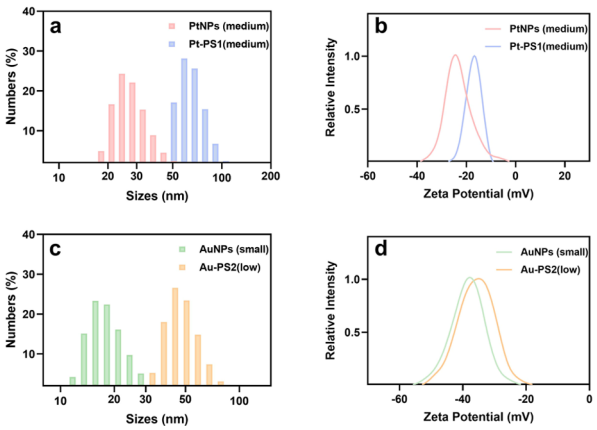


Figure 2. DLS and zeta potential characterization of reporter probes Pt-PS1 and Au-PS2. (a) DLS characterization of Pt-PS1 (medium). (b) Zeta potential investigation of Pt-PS1 (medium.) (c) DLS measurement for Au-PS2 (low). (d) Zeta potential characterization of Au-PS2 (low).

Prior to its implementation, it is imperative to verify that there is no cross-reactivity or unintended cross-linking between Cas12a and Cas13a, preventing them from mistakenly cleaving each other's designated probes. As depicted in Figure 3a, the activation of CRISPR-Cas12a by ctDNA selectively removes the PS1 DNA band, without altering the PS2 RNA band, emphasizing Cas12a's specific cleavage activity toward the PS1 DNA. In the meantime, Figure 3b displays a similar specificity phenomenon, where miRNA-activated CRISPR-Cas13a selectively degrades the PS2 RNA band, without disturbing the PS1 DNA band, emphasizing that Cas13a specifically targets and degrades the PS2 RNA. The observations from Figure 3a,b indicate that CRISPR-Cas12a and CRISPR-Cas13a function independently, without disrupting each other's cleavage of specific probe sequences, lending preliminary support to the feasibility of this assay. Additionally, aiming to make a double verification of the practicality of our protocol, which utilizes ICP-MS as the foundation for a biosensing platform capable of simultaneous detection of ctDNA and miRNA, we prepared a series of target gene fragments and subjected them to ICP-MS analysis. As presented in Figure 3c, the absence of both ctDNA and miRNA yields no signal response, but the presence of one or both triggers a high signal response, with dual high signals from ^{195}Pt and ^{197}Au observed when both are present, underscoring its cross-reactivity and confirming the practicality of this assay.

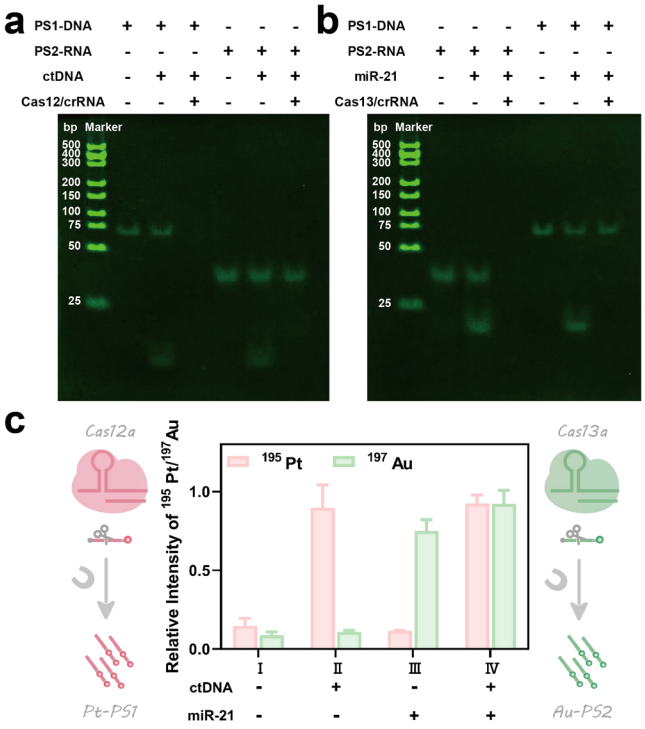


Figure 3. Assessment of feasibility. (a) Gel electrophoresis characterization of the *trans*-cleavage ability of CRISPR-Cas12a activated by a target against the substrate of PS1 DNA or PS2 RNA. (b) Gel electrophoresis characterization of the *trans*-cleavage ability of CRISPR-Cas13a activated by a target against the substrate of PS1 DNA or PS2 RNA. (c) Validation of the cross-reactivity between CRISPR-Cas12a and CRISPR-Cas13a by ICP-MS.

Optimization of Experimental Conditions. *Optimization of the Composition of Reporter Probes.* The reporter probes, Pt-PS1 and Au-PS2, serving as the substrate for CRISPR-Cas12a/Cas13a cleavage, are indispensable for signal transmission. The intensity of the signal output is closely tied to the size of the nanoparticles, and the distribution of PS1 DNA and PS2 RNA loaded onto them significantly dictates the amount of PtNPs and AuNPs that are liberated from the probes Pt-PS1 and Au-PS2. This distribution also affects the separation of uncleaved reporter probes from magnetic beads for signal isolation postreaction. As depicted in Figure 4a, the optimal modification density of PS1 DNA, which falls in the middle range, consistently enhances performance across different PtNP sizes. An excess of PS1 DNA may prevent complete Pt-PS1 cleavage when CRISPR-Cas12a is not fully activated by low target concentrations, thus impeding PtNP

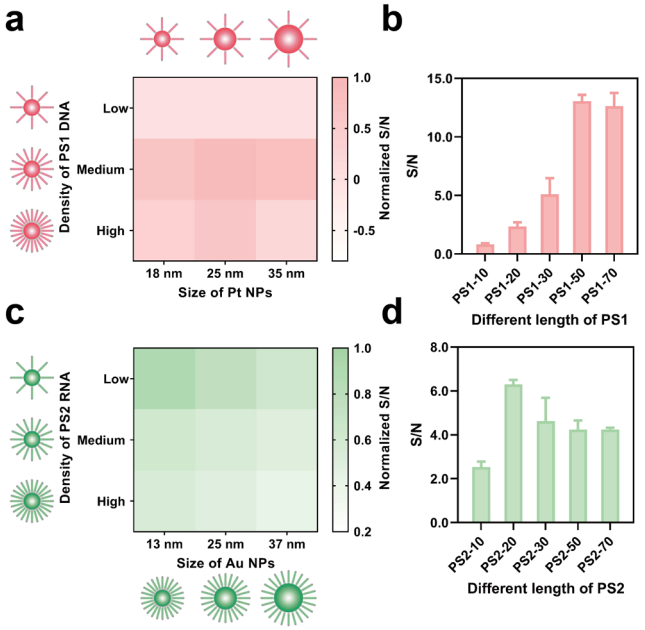


Figure 4. Enhancing the performance of reporter probes. (a) Assessing Pt-PS1 probes' performance across PtNPs sizes and PS1 DNA densities. (b) Maximizing Pt-PS1 probe efficiency via PS1 DNA length adjustment. (c) Comparing Au-PS2 probes' performance across AuNPs sizes and PS2 RNA densities. (d) PS2 RNA length optimization for enhanced Au-PS2 probe sensitivity.

https://doi.org/10.1021/acs.analchem.4c05961
Anal. Chem. XXXX, XXX, XXX−XXX

release. In contrast, insufficient PS1 DNA makes it difficult to bind the probes to the magnetic beads, hindering the ability to effectively separate signals and resulting in a higher background signal and lower signal quality. The Pt-PS1 (medium), with medium-sized PtNPs, and adorned with medium PS1 DNA density, emerged as the optimal choice for the CRISPR-Cas12a-ctDNA detection system (Cas12a-ctDNA). Smaller probes were limited by metal atom count, while larger ones suffered from excessive background noise, detracting from performance.

Another factor that impacts the performance of Pt-PS1 is the length of the PS1 DNA. A PS1 length that is too short can lead to excessive steric hindrance, which can impede Cas12a's cleavage ability. Through optimization, it was found that a PS1 length of 50 nt maximizes the signal-to-noise ratio (S/N), as depicted in Figure 4b. Surprisingly, 20 nt PS2 RNA in Au-PS2 probes shows the best S/N (Figure 4d), suggesting that Cas13a may be less vulnerable to steric hindrance than Cas12a. Across the CRISPR-Cas13a-miRNA detection system (Cas13a-miRNA), probes Au-PS2, regardless of the particle size of the AuNPs, consistently displayed superior performance when modified with low-density PS2 RNA, with those prepared with small AuNPs showing the best results (Figure 4c). The inconsistency between Cas12a-ctDNA and Cas13a-miRNA systems' optimal probes may lie in the longer length of PS1 DNA compared to PS2 RNA. Since both DNA and RNA are flexible, they tend to wrap around and fall onto the surface of nanoparticles as their length increases, reducing the number of exposed biotin sites for binding to magnetic beads. Therefore, in Cas12a-ctDNA, medium-density DNA probes perform best. In contrast, Cas13a-miRNA's short 20 nt PS2 RNA mostly remains upright, exposing more biotin sites for binding to magnetic beads, thereby favoring probes modified with low-density RNA.

Optimization of Dilution Ratios for Reporter Probes. The selection of the appropriate dilution ratio for the reporter probes Pt-PS1 and Au-PS2 is crucial for enhancing experimental performance. Too much probe can elevate background signals, while too little can diminish the desired signal intensity. For Pt-PS1, a 1:1 dilution offers the optimal S/N (Figure 5a), whereas Au-PS2 performs best at a 1:3 dilution (Figure 5b).

Optimization of the Amount of Cas12a/Cas13a. The amount of Cas proteins is a decisive factor in regulating the vigor and productivity of the cleavage reaction. Insufficient Cas proteins may hinder the complete cleavage of the reporter probe, resulting in a weakened signal. On the other hand, excess Cas proteins can trigger elevated background interference. As illustrated in Figure 5c,d, the ideal amount for Cas12a is 0.25 μL, whereas for Cas13a, it is 0.35 μL.

Optimization of the Ratio for Cas Proteins and crRNA. It is commonly acknowledged that CRISPR-Cas12a and CRISPR-Cas13a are both directed by crRNA to recognize and bind to their respective targets, resulting in the formation of a "Cas12a/crRNA/ctDNA" or "Cas13a/crRNA/miRNA" ternary structure that activates the respective Cas enzymes for efficient collateral cleavage. To expedite this process, an ample supply of crRNA is often necessary. However, excessive crRNA can lead to premature binding of individual crRNA molecules to the target, blocking the formation of the ternary complex with Cas proteins and consequently weakening the signal. Experimental evidence points to a 1:4 Cas12a to crRNA1 ratio as optimal (Figure 5e), whereas for Cas13a, a 1:2 Cas13a to crRNA2 ratio achieves the best performance (Figure 5f).

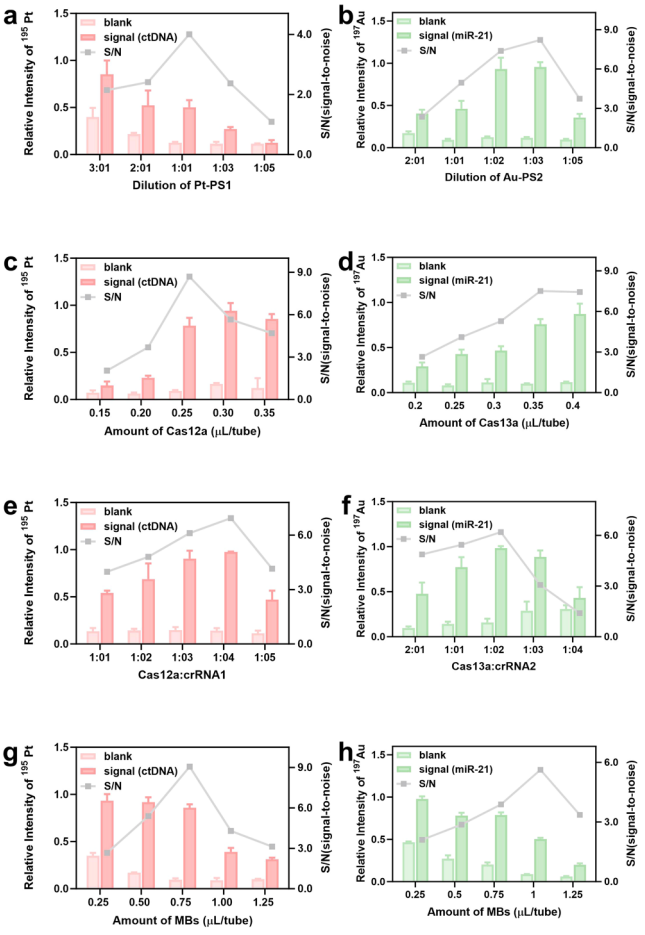


Figure 5. Optimization of various experimental conditions. (a) Optimization of the dilution ratio for the reporter probe Pt-PS1. (b) Optimization of the dilution ratio for the reporter probe Au-PS2. (c) Comparison of Cas12a performance with varying dosages. (d) Comparison of Cas13a performance with varying dosages. (e) Optimization of the ratio between Cas12a and crRNA1. (f) Optimization of the ratio between Cas13a and crRNA2. (g) Optimization of the amount of MBs for Pt-PS1 separation in the Cas12a-ctDNA system. (h) Optimization of the amount of MBs for Au-PS2 separation in the Cas13a-miRNA system.

Optimization of Other Factors Impacting Cas Proteins' Cleavage Efficacy. The Mg^{2+} concentration in the reaction buffer is crucial for maintaining the correct folding of crRNA and initiating the *trans*-cleavage mechanism of Cas12a/Cas13a, while the reaction temperature and time are essential parameters that amplify the effectiveness of these enzymes. Considering all factors, a Tris-HCl buffer with 10 mM Mg^{2+}, conducted at 37 °C for 40 min, is advised for the simultaneous detection of ctDNA and miRNA (Figure S7).

Optimization of the Amount of MBs. The amount of MBs is paramount in differentiating the Cas-mediated cleavage signals from those of intact reporter probes. Insufficient MBs hinder efficient separation, while excessive MBs can compromise signal intensity by attracting nanoparticles nonspecifically, diminishing their release into the supernatant. Our data indicate that 0.75 μL of MBs per tube is optimal for Cas12a-ctDNA assays (Figure 5g), and 1 μL of MBs yields the best S/N for Cas13a-miRNA detection (Figure 5h). Consequently, a

https://doi.org/10.1021/acs.analchem.4c05961
Anal. Chem. XXXX, XXX, XXX−XXX

combined 1.75 μL of MBs per tube is proposed for subsequent experiments, allowing simultaneous Cas12a/Cas13a-mediated analysis of ctDNA and miRNA, while efficiently segregating residual Pt-PS1 and Au-PS2 probes.

Analytical Performance of Simultaneous Detection of ctDNA and miRNA. Upon utilizing the previously optimized experimental parameters, we examined the analytical capabilities of the CRISPR-Cas12a/Cas13a system for the simultaneous quantification of ctDNA and miRNA. By introducing various concentrations of ctDNA and miR-21 to activate Cas12a and Cas13a, respectively, these enzymes execute *trans*-cleavage on their corresponding probes Pt-PS1 and Au-PS2, resulting in the release of PtNPs and AuNPs, respectively. The quantity of nanoparticle liberation is reflected in the dual peaks of ^{195}Pt and ^{197}Au detected by ICP-MS. As shown in Figure 6a,b, within a certain range of concentrations,

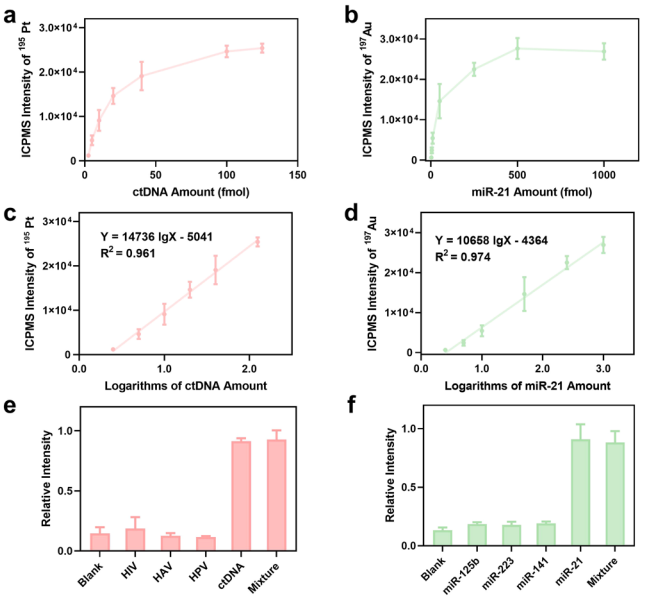


Figure 6. Analytical performance and selectivity. (a) ^{195}Pt signal response to varying amounts of ctDNA. (b) ^{197}Au signal response to varying amounts of miR-21. (c) Linear logarithmic relationship between the ^{195}Pt signal intensity and the ctDNA concentration. (d) Linear logarithmic relationship between the ^{197}Au signal intensity and the miRNA concentration. (e) Selectivity and specificity of the Cas12a-ctDNA system. (f) Selectivity and specificity of the Cas13a-miRNA system.

the intensities of ^{195}Pt and ^{197}Au increase proportionally with the augmentation of added ctDNA and miRNA, respectively. Specifically, for the Cas12a-ctDNA system, the ^{195}Pt signal intensity demonstrated a robust linear logarithmic correlation with the concentration of ctDNA ranging from 2.5 to 125 fmol, adhering to the equation y = 14,736 lg x (fmol) − 5041. Notably, the limit of detection (LOD, calculated as 3σ/k) was exceptionally low at 1.1 fmol (Figure 6c and Table 1).[45,46] Similarly, in the Cas13a-miRNA system, the ^{197}Au signal intensity correlated linearly and logarithmically with the miR-21 concentration over the range of 2.5−1000 fmol, adhering to the equation y = 10,658 lg x (fmol) − 4364, with an LOD of 1.0 fmol (Figure 6d and Table 1). The integration of CRISPR-Cas12a/Cas13a and ICP-MS as the signal transduction platform for the simultaneous quantification of ctDNA and miRNA exhibits exceptional quantitative analytical abilities. This is attributed to the potent trans-cleavage function of CRISPR-Cas12a/Cas13a and the unparalleled strengths of ICP-MS, including its superior capacity for multielement analysis and immunity to spectral interference. Apart from that, we evaluated the analytical performance of our proposed method against other recent amplification-based assays for quantifying ctDNA and miR-21 (Table S3),[47,48] as well as dual-amplification systems that integrate CRISPR with other amplification protocols (Table S4).[49,50] Encouragingly, our method's performance is mostly superior or comparable, suggesting that its integration with amplification technologies in the future may pave the way for even more sensitive simultaneous detection of ctDNA and miRNA, enabling the examination of complex clinical samples and contributing to early disease diagnosis.

Specificity and Serum Assay. In order to assess the selectivity and specificity of our proposed analytical methodology, we compared the signal intensities of the CRISPR-Cas12a/Cas13a systems with target concentrations (50 fmol ctDNA for Cas12a, 500 fmol miR-21 for Cas13a) and interfering substances at 10-fold higher concentrations. For the CRISPR-Cas12a system, HIV, HAV, and HPV are selected as the interfering substances, and for the CRISPR-Cas13a system, miR-125b, miR-223, and miR-141 are employed. Figure 6e,f clearly shows that the signal response remains subdued, even in the presence of interferents at concentrations much higher than the target. Furthermore, even when the CRISPR-Cas12a/Cas13a systems are activated with a mixture containing the target at its native concentration and interferents at 10 times that concentration, the resulting signal intensity is comparable to that observed with the target alone, emphasizing the favorable selectivity and specificity of our analytical methodology. To assess the practical viability of our analytical method, we conducted spiked recovery assays on human serum samples. Herein, we spiked a range of concentrations of ctDNA and miR-21 into different serum samples and subsequently analyzed them. The results, summarized in Table S5, show recovery rates ranging from 93.1 to 108.3%, with RSD varying from 1 to 7.9%. This affirms the promising potential of our method, which employs CRISPR-Cas12a/Cas13a and ICP-MS as signal transduction platforms, for the simultaneous quantification of ctDNA and miRNA in complex clinical samples.

CONCLUSIONS

In summary, we developed a simple and rapid mass spectrometry method that leverages CRISPR-Cas12a/Cas13a and ICP-MS in conjunction with freeze-labeled nanoparticles as signal reporters for simultaneous analysis of ctDNA and miRNA. The potent *trans*-cleavage function of CRISPR-

Table 1. Analytical Performance for the Simultaneous Detection of ctDNA and miRNA

detection method	target	liner range (fmol)	liner relationship	LOD (fmol)
CRISPR-Cas12a	ctDNA	2.5−125	y = 14,736 lg x (fmol) − 5041	1.1
CRISPR-Cas13a	miR-21	2.5−1000	y = 10,658 lg x (fmol) − 4364	1.0

https://doi.org/10.1021/acs.analchem.4c05961
Anal. Chem. XXXX, XXX, XXX−XXX

Cas12a/Cas13a, ICP-MS unparalleled sensitivity and versatility in multielement analysis, as well as the nanoparticle intrinsic self-amplification facilitate ultrahigh sensitivity detection of ctDNA and miRNA, eliminating the requirement for further nucleic acid amplification. Furthermore, this method demonstrates favorable specificity and potential for further clinical applications, positioning it as a promising platform for integrated diagnostic-therapeutic systems aimed at early disease detection.

■ ASSOCIATED CONTENT

Supporting Information

The Supporting Information is available free of charge at https://pubs.acs.org/doi/10.1021/acs.analchem.4c05961.

Materials and reagents, apparatus, buffers, all nucleic acid sequences used in this study, and working parameters of ICP-MS; synthesis of nanoparticles and DLS characterization of PtNPs and AuNPs; DLS, zeta potential, and UV spectroscopy used to characterize the reporter probes Pt-PS1 and Au-PS2, composed of varying sizes and loaded with low, medium, and high PS1 DNA or PS2 RNA densities; optimization of additional experimental conditions; comparison of the analytical performance of this work with other amplification methods or amplification techniques incorporating CRISPR; and recovery of ctDNA and miR-21 from human serum samples (PDF)

■ AUTHOR INFORMATION

Corresponding Authors

Rui Liu − *Key Laboratory of Green Chemistry and Technology, Ministry of Education, College of Chemistry, Sichuan University, Chengdu 610064 Sichuan, China;* orcid.org/0000-0001-9928-5373; Phone: +86-28-8541-2398; Email: liur@scu.edu.cn; Fax: +86-28-8541-2398

Yi Lv − *Key Laboratory of Green Chemistry and Technology, Ministry of Education, College of Chemistry and Analytical and Testing Center, Sichuan University, Chengdu 610064 Sichuan, China;* orcid.org/0000-0002-7104-2414; Phone: +86-28-8541-2798; Email: lvy@scu.edu.cn; Fax: +86-28-8541-2798

Authors

Yan Li − *Key Laboratory of Green Chemistry and Technology, Ministry of Education, College of Chemistry, Sichuan University, Chengdu 610064 Sichuan, China*

Yichen Li − *Key Laboratory of Green Chemistry and Technology, Ministry of Education, College of Chemistry, Sichuan University, Chengdu 610064 Sichuan, China*

Yueli Hu − *Key Laboratory of Green Chemistry and Technology, Ministry of Education, College of Chemistry, Sichuan University, Chengdu 610064 Sichuan, China*

Complete contact information is available at: https://pubs.acs.org/10.1021/acs.analchem.4c05961

Notes

The authors declare no competing financial interest.

■ ACKNOWLEDGMENTS

The work was greatly supported by the National Natural Science Foundation of China (No. 22374105), the Sichuan Science and Technology Program (No. 2025NSFTD0001), the Talents Program of Sichuan Province (No. 903), and the Fundamental Research Funds for the Central Universities. Dr. Jing Zhou and Dr. Xiaobin Xie from the Analytical and Testing Center, Sichuan University, are gratefully thanked for their invaluable contributions and technical support.

■ REFERENCES

(1) Zeng, R.; Gong, H.; Li, Y.; Li, Y.; Lin, W.; Tang, D.; Knopp, D. *Anal. Chem.* **2022**, *94* (20), 7442−7448.

(2) Li, Y.; Zeng, R.; Wang, W.; Xu, J.; Gong, H.; Li, L.; Li, M.; Tang, D. *ACS Sens.* **2022**, *7* (5), 1593−1601.

(3) Makarova, K. S.; Haft, D. H.; Barrangou, R.; Brouns, S. J. J.; Charpentier, E.; Horvath, P.; Moineau, S.; Mojica, F. J. M.; Wolf, Y. I.; Yakunin, A. F.; et al. *Nat. Rev. Microbiol* **2011**, *9* (6), 467−477.

(4) Nuñez, J. K.; Chen, J.; Pommier, G. C.; Cogan, J. Z.; Replogle, J. M.; Adriaens, C.; Ramadoss, G. N.; Shi, Q. M.; Hung, K. L.; Samelson, A. J.; et al. *Cell* **2021**, *184* (9), 2503.

(5) Weng, Z. Y.; You, Z.; Yang, J.; Mohammad, N.; Lin, M. S.; Wei, Q. S.; Gao, X.; Zhang, Y. *Angew. Chem., Int. Ed.* **2023**, *62*, No. e202214987.

(6) Feng, W.; Newbigging, A. M.; Tao, J.; Cao, Y. R.; Peng, H. Y.; Le, C.; Wu, J. J.; Pang, B.; Li, J.; Tyrrell, D. L.; et al. *Chem. Sci.* **2021**, *12* (13), 4683−4698.

(7) Wang, K.; Xu, B. F.; Lei, C. Y.; Nie, Z. *J. Anal Test* **2021**, *5* (2), 130−141.

(8) Chen, J. S. *Science* **2021**, *371* (6531), 791.

(9) Gootenberg, J. S.; Abudayyeh, O. O.; Lee, J. W.; Essletzbichler, P.; Dy, A. J.; Joung, J.; Verdine, V.; Donghia, N.; Daringer, N. M.; Freije, C. A.; et al. *Science* **2017**, *356* (6336), 438−442.

(10) Yuan, A. J.; Sha, R.; Xie, W. J.; Qu, G. B.; Zhang, H. Q.; Wang, H. L.; Le, X. C.; Jiang, G. B.; Peng, H. Y. *J. Am. Chem. Soc.* **2024**, *146* (39), 26657−26666.

(11) Tang, Z. W.; Gao, M. L.; Gong, F.; Shan, X. Y.; Yang, Y. L.; Zhang, Y. R.; Chen, L. J.; Wang, F. B.; Ji, X. H.; Zhou, F. X.; et al. *Anal. Chem.* **2024**, *96* (40), 16017−16026.

(12) Tian, T.; Qiu, Z.; Jiang, Y.; Zhu, D.; Zhou, X. *Biosens Bioelectron* **2022**, *196*, No. 113701.

(13) Fu, J.; Zhang, L.; Long, Y.; Liu, Z.; Meng, G.; Zhao, H.; Su, X.; Shi, S. *Anal. Chem.* **2023**, *95* (44), 16089−16097.

(14) Gootenberg, J. S.; Abudayyeh, O. O.; Kellner, M. J.; Joung, J.; Collins, J. J.; Zhang, F. *Science* **2018**, *360* (6387), 439−444.

(15) Abudayyeh, O. O.; Gootenberg, J. S.; Kellner, M. J.; Zhang, F. *CRISPR J.* **2019**, *2* (3), 165−171.

(16) Xu, Z. C.; Chen, D. J.; Li, T.; Yan, J. Y.; Zhu, J.; He, T.; Hu, R.; Li, Y.; Yang, Y. H.; Liu, M. L. *Nat. Commun.* **2022**, *13* (1), 6480.

(17) Tang, C. H.; Dong, Z. Z.; Yan, S.; Liu, B.; Wang, Z. Y.; Cheng, L.; Liu, F.; Sun, H.; Du, Y. M.; Pan, L.; et al. *Biosens Bioelectron* **2025**, *267*, No. 116748.

(18) Wang, R.; Zhao, X.; Chen, X.; Qiu, X.; Qing, G.; Zhang, H.; Zhang, L.; Hu, X.; He, Z.; Zhong, D.; et al. *Anal. Chem.* **2020**, *92* (2), 2176−2185.

(19) Li, Z. Y.; Liu, R.; Lv, Y. *Appl. Spectrosc Rev.* **2023**, *58* (1), 39−64.

(20) Bodenmiller, B.; Zunder, E. R.; Finck, R.; Chen, T. J.; Savig, E. S.; Bruggner, R. V.; Simonds, E. F.; Bendall, S. C.; Sachs, K.; Krutzik, P. O.; et al. *Nat. Biotechnol.* **2012**, *30* (9), 858−U889.

(21) Virani, F.; Tanner, S. *Spectroscopy* **2015**, *30* (5), 14−22.

(22) Liu, R.; Wu, P.; Yang, L.; Hou, X.; Lv, Y. *Mass Spectrom Rev.* **2014**, *33* (5), 373−393.

(23) Liu, R.; Zhang, S. X.; Wei, C.; Xing, Z.; Zhang, S. C.; Zhang, X. R. *Acc. Chem. Res.* **2016**, *49* (5), 775−783.

(24) Xu, T. R.; Feng, D. S.; Li, H.; Hu, X. S.; Wang, T.; Hu, C. X.; Shi, X. Z.; Xu, G. W. *Trac-Trend Anal Chem.* **2022**, *157*, No. 116763.

(25) Liu, Z. R.; Li, X. T.; Xiao, G. Y.; Chen, B. B.; He, M.; Hu, B. *Trac-Trend Anal Chem.* **2017**, *93*, 78−101.

(26) Liang, Y.; Yang, L. M.; Wang, Q. Q. *Appl. Spectrosc Rev.* **2016**, *51* (2), 117−128.

(27) Wen, Y.; Zhang, X. W.; Li, Y. Y.; Chen, S.; Yu, Y. L.; Wang, J. H. *Anal. Chem.* **2022**, *94* (46), 16196−16203.
(28) Zhu, Y. L.; Lian, Y. M.; Wang, J. K.; Chen, Z. P.; Yu, R. Q. *Anal. Chem.* **2021**, *93* (14), 5839−5848.
(29) Kang, Q.; Chen, B. B.; He, M.; Hu, B. *Anal. Chem.* **2024**, *96* (16), 6329−6336.
(30) Chen, X.; Zhao, X.; Pu, S. R.; Liu, R.; Lv, Y. *Atom. Spectrosc.* **2023**, *44* (6), 427−433.
(31) Sun, G. W.; Huang, B.; Zhang, Y.; Zhang, Y. Q.; Xing, Z.; Zhang, S. C.; Zhang, X. R. *Chem. Commun.* **2017**, *53* (97), 13075−13078.
(32) Li, Y.; Huang, Z.; Li, Z.; Li, C.; Liu, R.; Lv, Y. *Anal. Chem.* **2022**, *94* (49), 17248−17254.
(33) Wang, C. Q.; Deng, Z. Q.; Zhang, H.; Liu, R.; Lv, Y. *Chin. Chem. Lett.* **2022**, *33* (3), 1267−1270.
(34) Li, B.-R.; Tang, H.; Yu, R.-Q.; Jiang, J.-H. *Anal. Chem.* **2021**, *93* (24), 8381−8385.
(35) Deng, Z. Q.; Hu, J. Y.; Liu, R.; Lv, Y. *Atom. Spectrosc.* **2022**, *43* (3), 201−206.
(36) Xu, Y.; Chen, B. B.; He, M.; Cui, Z. W.; Hu, B. *Anal. Chem.* **2023**, *95* (37), 14061−14067.
(37) Liu, M. J.; Wei, X.; Wu, C. X.; Liu, J. H.; Wei, Y. J.; Wang, X. S.; Chen, M. L.; Yang, T.; Wang, J. H. *Anal. Chem.* **2023**, *95* (38), 14447−14454.
(38) Zhou, Y.; Chen, Z. Q.; Zeng, J. X.; Zhang, J. X.; Yu, D. X.; Zhang, B.; Yan, X. W.; Yang, L. M.; Wang, Q. Q. *Anal. Chem.* **2020**, *92* (7), 5286−5293.
(39) Dang, J. Q.; Li, H. X.; Zhang, L. L.; Li, S. J.; Zhang, T.; Huang, S. Y.; Li, Y. Y.; Huang, C. J.; Ke, Y. Q.; Shen, G. X.; et al. *Adv. Mater.* **2021**, *33* (35), No. 2008297.
(40) Rupaimoole, R.; Slack, F. J. *Nat. Rev. Drug Discov* **2017**, *16* (3), 203−221.
(41) Stejskal, P.; Goodarzi, H.; Srovnal, J.; Hajduch, M.; Vant Veer, L. J.; Magbanua, M. J. M *Mol. Cancer* **2023**, *22* (1), 15.
(42) Lv, S.; Zhang, K.; Zeng, Y.; Tang, D. *Anal. Chem.* **2018**, *90* (11), 7086−7093.
(43) Lin, Y.; Zhou, Q.; Tang, D.; Niessner, O.; Knopp, D. *Anal. Chem.* **2017**, *89* (10), 5637−5645.
(44) Hu, M. L.; Yuan, C. Q.; Tian, T.; Wang, X. S.; Sun, J.; Xiong, E. H.; Zhou, X. M. *J. Am. Chem. Soc.* **2020**, *142* (16), 7506−7513.
(45) Zeng, R.; Xu, J.; Lu, L.; Lin, Q.; Huang, X.; Huang, L.; Li, M.; Tang, D. *Chem. Commun.* **2022**, *58*, 7562−7565.
(46) Wang, Y.; Zeng, R.; Tian, S.; Chen, S.; Bi, Z.; Tang, D.; Knopp, D. *Anal. Chem.* **2024**, *96* (33), 13663−13671.
(47) Hu, Y. Y.; Guo, X.; Gu, P. L.; Luo, Q.; Song, Y.; Song, E. Q. *Sensor Actuat B-Chem.* **2021**, *330*, No. 129340.
(48) Shi, L. J.; Li, J.; Xiang, Q.; Tan, Y. P.; Zhang, H. Y.; Liu, S. H.; Guo, X. Q.; Zhang, W. J.; Yang, D. Z.; Ma, Y. S. *Biosens Bioelectron* **2023**, *237*, No. 115529.
(49) Wu, X. L.; Ju, T.; Li, Z. Y.; Li, J. W.; Zhai, X. W.; Han, K. *Anal. Chim. Acta* **2023**, *1261*, No. 341170.
(50) Zhou, S. Y.; Liu, M. L.; Deng, L. Y.; Qiu, Y.; Gu, T.; Chen, J.; Yang, M.; Huo, D. Q.; Hou, C. J. *Sensor Actuat B-Chem.* **2024**, *408*, No. 135490.

https://doi.org/10.1021/acs.analchem.4c05961
Anal. Chem. XXXX, XXX, XXX−XXX